

A localized electrons detector for atomic and molecular systems

Hugo J. Bohórquez · Russell J. Boyd

Received: 19 November 2009 / Accepted: 14 January 2010 / Published online: 9 February 2010
© Springer-Verlag 2010

Abstract The *local value* of the single-particle momentum provides a direct three-dimensional representation of bonding interactions in molecules. It is given exclusively in terms of the electron density and its gradient, and therefore is an ideal localized electrons detector (LED). The results introduced here extend to molecular systems our study of the single-particle local momentum in atomic systems (Bohórquez and Boyd in *J Chem Phys* 129:024110, 2008; *Chem Phys Lett* 480:127, 2009). LED is able to clearly identify covalent and hydrogen bonding interactions by depicting distinctive regions around the bond critical points, emerging as a complementary tool in conventional *atoms in molecules* studies. The local variable we introduce here is an intuitively interpretable 3D electron-pairs locator in atoms and molecules that can be computed either from theoretical or experimentally derived electron densities.

Keywords Electron pairs · Electron localization · Chemical bond · Quantum topology · Electron momentum · Electron kinetic energy · Local quantum value · Theoretical methods

1 Introduction

“Sometimes it seems to me that a bond between two atoms has become so real, so tangible, so friendly, that I can almost see it. Then I awake with a little shock, for a chemical bond is not a real thing. It does

not exist. No one has ever seen one. No one ever can. It is a figment of our own imagination.” Charles A. Coulson

Electronic bonding interactions are not directly observable, as Coulson asserts, but our intuitive perception of molecular phenomena in the three-dimensional space demands such a representation. With a similar perspective Lewis conceived the idea of electron pairs [1]. It is reasonable to think that an adequate representation of chemical bonding should be given by a physical observable defined in coordinate space. The electron density is the best choice because it is a local function defined within the exact many-body theory, and it is also an experimentally accessible scalar field. Its paramount role in the description of many-body problems is supported by the Hohenberg–Kohn theorem [2].

Although the Hohenberg–Kohn theorem guarantees that all the molecular information is encoded in the electron density, the physical description of chemical systems requires additional postulates for extracting observable information in terms of atomic contributions. This is achieved by the quantum theory of atoms in molecules (QTAIM) introduced by Bader [3]. The *proper open system* concept provides a quantum topological partitioning of the molecular space into chemically transferable molecular fragments for which the energy and all other measurable properties can be precisely defined [4].

The localization of electron pairs is elusive within the electron density topology analysis, because a direct link between the local maxima in the electron density and the electron pairs of the Lewis model has not been established, despite the fact that the Laplacian of the electron density provides some information about electron localization [5]. Several attempts to depict electron localization from different perspectives have been proposed in recent years. The variety

H. J. Bohórquez (✉) · R. J. Boyd
Department of Chemistry, Dalhousie University,
Halifax, NS B3H 4J3, Canada
e-mail: hugo.j.bohorquez@dal.ca

of proposals for assessing that single task leads to the logical question of why the conventional analysis seems to be insufficient to fully explain electron localization in molecules.

We identify two main causes: one is interpretation, and the other is of a practical nature. The conventional analyses consist mainly of the study of the Laplacian of the electron density [6], and the electron localization function (ELF) [7]. Both approaches entail conceptual and practical limitations. The Laplacian provides information about local concentration or depletion of electron density, but its values are not bounded, and it fails to correctly produce atomic shells for atoms beyond the third row [8]. A direct link between ELF and QTAIM is still missing, whereas an homeomorphic relationship¹ with the Laplacian has been suggested [5].

The electron localization function, by construction, provides values within the [0, 1] range, and its topological analysis by Silvi and Savin [9] made ELF a preferred tool for the study of electronic bonding interactions. In spite of its formally sound derivation from the electronic pair probability, ELF interpretation is not straightforward and the respective plots are far from intuitively evident, a feature to be expected of an ideal representation of chemical bonding interactions. Additionally, ELF fails to provide insight for non-covalent bonding interactions, limiting even more its application for the study of unconventional bonding situations and weak intermolecular interactions.

In the present paper, we introduce a variable that has the ability to detect electron pairs inside an electron density distribution, and overcomes the limitations of the other analyses. Our localized electrons detector (LED) depends exclusively on the electron density and its gradient. Here we show how this variable consistently fits within the conventional atoms in molecules analysis, by providing complementary information about the physics of bonding interactions and their local symmetries. The present work extends to molecular systems our previous investigation of this local variable in atomic systems. We have shown that LED correctly provides atomic shell structures [10], and an atomic radius scale that can be experimentally derived [11], among other interesting results. Herein we illustrate its application to molecular systems.

In the following section, we examine the variables involved in ELF in order to show that its key ingredient is the single-particle kinetic energy density, which is connected to our LED by a quantum theorem (see Sect. III A in Ref. [10]). Several important features of this variable, including its bounded character, and its direct connection to QTAIM are discussed in the second part of Sect. 2. In Sect. 3, we show the results of the proposed analysis with several examples, showing how LED identifies the presence of electron shells,

and the different bonding interactions adequately. This graphical representation of bonding regions in coordinate space provides distinctive graphical representations for covalent and hydrogen bonding interactions as well.

In summary, LED provides an orbital-free and intuitively interpretable three-dimensional electron-pair localization scalar function that is easy to compute from either theoretically computed or experimentally derived electron densities.

2 Theoretical considerations

In this section, we show that the single-particle kinetic energy local momentum $\tilde{\mathbf{P}}$ is linked to one of ELF's key components, as an alternative to its derivation introduced in Ref. [10] from the local quantum theory [12].

The ELF was introduced by Becke and Edgecombe [7] as a “simple measure of electron localization in atomic and molecular systems”. Two terms of a Taylor series expansion of the spherically averaged conditional same-spin pair probability density provide the main ELF equation, i.e. the kinetic energy density variable

$$\mathcal{D}(\mathbf{r}) = \tau(\mathbf{r}) - \kappa(\mathbf{r}) \quad (1)$$

where the first term is the orbital or positive-definite kinetic energy density

$$\tau(\mathbf{r}) = \frac{\hbar^2}{2m_e} \sum_i |\nabla \psi_i(\mathbf{r})|^2 \quad (2)$$

and the second term is the single particle or von Weizsäcker kinetic energy density

$$\kappa(\mathbf{r}) = \frac{\hbar^2}{8m_e} \frac{\nabla \rho(\mathbf{r}) \cdot \nabla \rho(\mathbf{r})}{\rho(\mathbf{r})} \quad (3)$$

\mathcal{D} in Eq. 1 is proportional to the Fermi hole mobility function of Luken and Culberson [13] and is related to the curvature of the Fermi hole as shown by Dobson [14]. Becke and Edgecombe identify the localization of an electron with the probability density to find an electron in the vicinity of a second same-spin reference electron. The smaller the probability density \mathcal{D} , the higher the localization of the electrons. In order to get values in the range from 0 to 1, ELF is defined as the Lorentzian mapping (\mathcal{L}) of the core variable χ , i.e.

$$\eta(\mathbf{r}) \doteq \mathcal{L}(\chi(\mathbf{r})) = \frac{1}{[1 + \chi^2(\mathbf{r})]} \quad (4)$$

with $\chi(\mathbf{r}) = \mathcal{D}(\mathbf{r})/\mathcal{D}_h(\mathbf{r})$, where

$$\mathcal{D}_h(\mathbf{r}) = \frac{3\hbar^2}{5m_e} (6\pi^2)^{2/3} \rho(\mathbf{r})^{5/3} \quad (5)$$

is the kinetic energy density of the free electron gas associated with the electron density ρ .

¹ Two functions are said to be homeomorphic if one can be continuously transformed into the other.

Becke and Edgecombe interpreted the ratio χ as a convenient dimensionless localization index calibrated with respect to the uniform electron gas.² In this sense, ELF is a local measure of the effect of the Pauli exclusion principle as reflected by the kinetic energy density: in the regions of space where this effect is smaller than the kinetic energy density of a uniform electron gas of identical density, ELF is close to 1, whereas where the local parallel spin pairing is higher, ELF is low.

But the only measure of the electron localization present in ELF is the expression \mathcal{D} , as was recently pointed out by Gatti [15]. However, he adds, ELF cannot yield the value of \mathcal{D} because its dependence on the electron density via the free electron gas term \mathcal{D}_h . In this sense, ELF is a *relative* measure of the electron localization. It is, in fact, a relative measure of the *bosonic character* of the electron density, because \mathcal{D} is the excess kinetic energy electrons have compared to a system of bosons of the same density. This interpretation of ELF was introduced by Silvi and Savin [16], who also introduced a generalized kinetic density version of ELF and its topological analysis [9].

In order to illustrate these observations, the variables involved in ELF are plotted in Fig. 1 for the bonding ($\mathbf{r} \in [\mathbf{r}_{BCP}, \mathbf{R}_F]$) and non-bonding regions ($\mathbf{r} > \mathbf{R}_F$) of fluorine molecule, where $\mathbf{r}_{BCP} = 0$ is the position of the bond critical point (BCP), and the fluorine nucleus is located at $\mathbf{R}_F = 1.35$ a.u. In Fig. 1 these two points are indicated at the top. Figure 1a shows the *local values*³ of the variables involved in \mathcal{D} , τ/ρ (in blue) and κ/ρ (in purple). Figure 1b shows the Lorentzian mapping of the local variable⁴ \mathcal{D}/ρ , $\mathcal{L}(\mathcal{D}/\rho)$ (in green), and the ELF, η (in red).

The two electron shells of fluorine are clearly visible with κ/ρ and \mathcal{D}/ρ , while ELF is unable to depict them. Even $\mathcal{L}(\mathcal{D}/\rho)$ shows more clearly than η the location of core electrons from the valence electrons, in accordance with Gatti's observation. The local value of the single particle kinetic energy, κ/ρ , provides additional chemical information not given by the other variables: the location of the BCP at $\kappa/\rho = 0$, which is relevant for the study of topological properties in molecules; and the polarization of non-bonding regions, which is relevant for intermolecular interactions studies.

² This is an arbitrarily chosen reference variable, found also in the Fermi hole mobility function by Luken and Culberson [13], but instead of a division they made a subtraction, also arbitrarily choosing the uniform electron gas as a reference. While this choice seems physically sound, valence electrons behave as a non-interacting electron gas in crystals mainly and therefore its inclusion in other molecular systems is not entirely justified.

³ These are bounded variables unlike their respective kinetic densities, τ and κ , and have units of energy per particle, not energy per volume. For more details on the local values in quantum chemistry, see Ref. [10] and references therein.

⁴ It means, replacing \mathcal{D}/ρ instead of χ in Eq. 4.

Electron pairs are stable groups of electrons that unlike free electrons, have integer spin and therefore behave as *composite bosons*. Atomic shells and covalent bonding interactions fit within that description. Recently, the bosonic character of electron pairs was experimentally confirmed [17]. A localized pair behaves as a single particle, and therefore its kinetic energy is given by the von Weizsäcker kinetic energy, κ . Therefore, its local value (κ/ρ) detects those regions of space where the molecule exhibits a marked single-particle character, providing in this way a direct measure of electron pairing. Consequently, this function is able to identify electron shells and covalent bonding interactions. Hence we propose the study of the bosonic character of atomic and molecular electron densities as a direct measure of their localized pairs.

A closer examination of κ/ρ depicted in Fig. 1 for di-fluorine reveals the existence of four different regions that can be identified going from the BCP to a long distance from the nucleus (~ 10 a.u.), along the molecular axis:

- The interatomic bonding region, characterized by a continuous approach of $\kappa/\rho \rightarrow 0$ as $\mathbf{r} \rightarrow \mathbf{r}_{BCP}$, and $\tau \gg \kappa$. A local maximum value in κ/ρ is located between the BCP and the core region.
- The core electron region is characterized by a continuous approach of κ/ρ to its absolute maximum, $\kappa/\rho \rightarrow Z^2/2$ (in a.u.) as $\mathbf{r} \rightarrow \mathbf{R}_A (\mathbf{r} \neq \mathbf{R}_A)$.⁵
- A non-bonding region, characterized by a local maximum in κ/ρ for which the outer zone of the valence shell is polarized and where $\tau \approx \kappa$.
- A molecular boundary region that is characterized by the asymptotic limit $\kappa \rightarrow \tau$, i.e. κ/ρ has a limiting value that depends on the molecular ionization energy.⁶

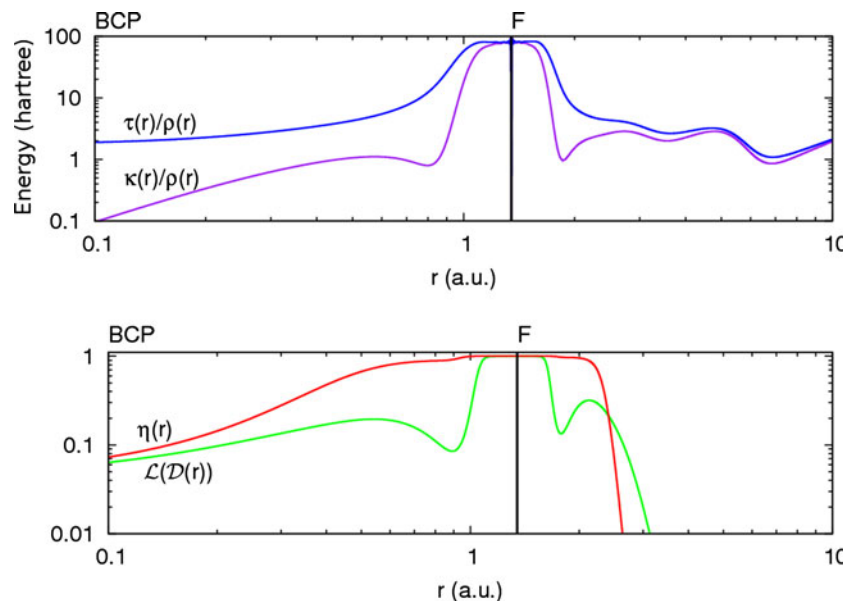
These four distinct regions can be identified in any pair of atoms connected by a gradient path within a molecule. Here we are interested in the first three mainly, because its direct relation with the presence of bonding interactions. Hence, the limiting values of \tilde{P} define three different spatial regions chemically relevant for the study of any molecular system: *covalent* ($\tilde{P} \simeq 0$), located around a BCP, *core* ($\tilde{P} \lesssim Z_A p_o$), located around the nuclear attractors, and *valence* regions ($\sqrt{2m_e I_Z} \lesssim \tilde{P} \ll Z p_o$),⁷ which includes polarized regions and valence shell electrons around the nucleus with atomic number Z .

⁵ Notice that at the nucleus there is a critical point of the electron density and hence $\kappa(\mathbf{R}_A) = 0$, but the neighbor points obey the limit.

⁶ Gaussian functions exhibit difficulties for reproducing the exponential decay, and therefore this limiting behavior is very sensitive to basis set selection [18].

⁷ Hydrogen is the only atom for which this relationship does not apply because $\sqrt{2m_e I_Z} = 1.4142$ a.u., which may be a consequence of its lack of an inner closed shell.

Fig. 1 Variables involved in ELF for the ground state of F_2 . Top local values τ/ρ and κ/ρ in coordinate space. Bottom ELF η and the Lorentzian map of the local value \mathcal{D}/ρ , $\mathcal{L}(\mathcal{D}/\rho)$ in coordinate space. The BCP is located at the left side of the graphic, and the figure is centered at the fluorine atom



Although we make reference to the kinetic energy τ , no explicit knowledge of this property is necessary for the bonding analysis provided by the single particle local value κ/ρ , as we show in the next section.

2.1 The single particle kinetic energy density and QTAIM

In our study of the single particle operators in atomic systems [10], we have shown that the expectation value of the single particle kinetic energy density, $\langle \kappa \rangle$, is equivalent to the variance of the momentum operator, $\mathbf{P} = -i\hbar\nabla$, minus its classical estimate $\overline{\mathbf{P}}$, i.e.

$$\kappa(\mathbf{r}) = \frac{1}{2m_e} \text{Var}_\psi(\mathbf{P} - \overline{\mathbf{P}}) \quad (6)$$

where $\widetilde{\mathbf{P}} \equiv \mathbf{P} - \overline{\mathbf{P}}$ is the fluctuation of the electronic momentum, whose single-particle expression applied to the electron density gives [10, 12, 19]

$$\widetilde{\mathbf{P}}(\mathbf{r}) = -\frac{\hbar}{2} \frac{\nabla \rho(\mathbf{r})}{\rho(\mathbf{r})} \quad (7)$$

which leads to

$$\langle \kappa(\mathbf{r}) \rangle = \int \frac{\widetilde{\mathbf{P}}(\mathbf{r}) \cdot \widetilde{\mathbf{P}}(\mathbf{r})}{2m_e} \rho(\mathbf{r}) d\mathbf{r} \quad (8)$$

This equation implies that κ/ρ can be expressed in terms of the local momentum component $\widetilde{\mathbf{P}}$ by $\kappa/\rho = \widetilde{\mathbf{P}} \cdot \widetilde{\mathbf{P}}/2m_e$. This means that $\widetilde{\mathbf{P}}$ provides at least the same information as κ/ρ . Additional information arises from the fact that $\widetilde{\mathbf{P}}$ is a vector variable.

The vector field (Eq. 7) $\widetilde{\mathbf{P}}$ points in the direction of maximum decrease in the electron density, and its magnitude \widetilde{P} is sensitive to local charge depletion. We have

found that atomic shells are limited by the radial distances from the nucleus where a change in the concavity of \widetilde{P} occurs, i.e. distances for which the condition $\partial^2 \widetilde{P} / \partial r^2 = 0$ is satisfied [10]. The electronic-shell populations are in excellent agreement with those obtained with ELF [20] and τ [21, 22], confirming the robustness of \widetilde{P} for depicting electron pairs in atoms.

For graphical analysis purposes, it is also convenient that \widetilde{P} is totally bounded by physically meaningful values. The lowest limit occurs at those points where the critical points of the electron density are located, i.e. for all those points that obey $\widetilde{P} = 0$. Kato's cusp condition imposes a limit to electron velocities near the nucleus of an atom A [23], \mathbf{R}_A , making \widetilde{P} finite and numerically equal to the atomic number Z_A , when atomic units are used.⁸

$$\lim_{\mathbf{r} \rightarrow \mathbf{R}_A} \widetilde{P}(\mathbf{r}) = p_0 Z_A \quad (9)$$

This velocity is used in the estimation of relativistic corrections for atomic systems [24]. Valence electron speeds in atoms are limited by the ionization energy I_A [10]

$$\lim_{|\mathbf{r}| \rightarrow \infty} \widetilde{P}(\mathbf{r}) = \sqrt{2m_e I_A} \quad (10)$$

This equation determines a natural boundary for an atom that leads to an experimentally based atomic radii scale [11]. Given the general validity of the exponential decay, it is expected that molecular regions depicted by $\widetilde{P}(\mathbf{r})$ are similarly bounded.

\widetilde{P} exhibits some additional practical advantages for topological analysis. In particular, it has a direct connection with the local variables studied in QTAIM, as we anticipated in Ref. [10]. This vector field runs anti-parallel to the

⁸ $p_0 = \hbar/a_0$ is the atomic unit of momentum.

gradient of the electron density $\nabla\rho$, hence depicting the same electron density gradient paths, but with opposite direction, i.e. they have opposite direction tangent vectors at every given point of the 3D space: $\nabla\rho/|\nabla\rho| = -\tilde{\mathbf{P}}/|\tilde{\mathbf{P}}|$. The gradient paths of the electron density connect the nuclei with BCPs, giving rise to an operative definition of molecular structure [25].

The electron density gradient field $\nabla\rho$ can be interpreted as the fluctuation of the current density vector field $\tilde{\mathbf{J}} = \frac{1}{m_e}\tilde{\mathbf{P}}\rho$, or equivalently

$$\tilde{\mathbf{J}}(\mathbf{r}) = -\frac{\hbar}{2m_e}\nabla\rho(\mathbf{r}) \quad (11)$$

The local flux of the current density fluctuation $\tilde{\mathbf{J}}(\mathbf{r})$ is given by the divergence operator,

$$\nabla \cdot \tilde{\mathbf{J}}(\mathbf{r}) = -\frac{\hbar}{2m_e}\nabla^2\rho(\mathbf{r}) = \frac{2}{\hbar}L(\mathbf{r}) \quad (12)$$

This equation indicates that the Laplacian of the electron density, L , effectively identifies local concentrations or depletion of electron density, just as QTAIM prescribes [3, 26].

There are two forces governing chemical structures, the Feynman force exerted on the nuclei and the Ehrenfest force exerted on the electrons. The virial theorem relates the virial of the Ehrenfest force to the kinetic energy of the electrons, the virial including a contribution from the virial of the Feynman forces acting on the nuclei. The local virial theorem is given in terms of the Laplacian of the electron density by Bader [3]

$$L(\mathbf{r}) = -2G(\mathbf{r}) - \mathcal{V}(\mathbf{r}) \quad (13)$$

or equivalently in terms of the current fluctuation (Eq. 11),

$$\frac{\hbar}{2}\nabla \cdot \tilde{\mathbf{J}}(\mathbf{r}) = -2G(\mathbf{r}) - \mathcal{V}(\mathbf{r}) \quad (14)$$

where $G(\mathbf{r})$ is the positively defined kinetic energy density, and $\mathcal{V}(\mathbf{r})$ is the virial density.

The integral form of the virial, $-2G = \mathcal{V}$, requires that the net flux of the current density vanish, which is granted by the divergence theorem applied to the current density

$$\int \nabla \cdot \tilde{\mathbf{J}}(\mathbf{r}) d\mathbf{r} = \oint \tilde{\mathbf{J}}(\mathbf{r}) \cdot \mathbf{n} ds = 0 \quad (15)$$

In order to make this condition valid for any given atomic basin region, Ω , the local flux of the current density $\tilde{\mathbf{J}}$ over the surface of this region ($\partial\Omega$) must vanish, which leads to the local zero-flux condition at the interatomic surface⁹

$$\tilde{\mathbf{J}}(\mathbf{r}_{\partial\Omega}) \cdot \mathbf{n}(\mathbf{r}_{\partial\Omega}) = 0 \quad (16)$$

that finally gives, after using Eq. 11,

⁹ A similar derivation is discussed by Delle Site in Ref. [27].

$$\nabla\rho(\mathbf{r}_{\partial\Omega}) \cdot \mathbf{n}(\mathbf{r}_{\partial\Omega}) = 0 \quad (17)$$

which defines those points $\mathbf{r}_{\partial\Omega}$ located on the basin surface $\partial\Omega$. The molecular space can be exhaustively partitioned into the atomic basins defined by Eq. 17, as stated by QTAIM.

Equations 11–17 show that $\tilde{\mathbf{P}}$ is consistent with QTAIM definitions of structure in terms of bond paths and that of proper open system. Additionally, and this is the main claim made here, $\tilde{\mathbf{P}}$ also reveals the single-particle character of localized electrons within the electron density by depicting the atomic shell structures and the symmetry of bonding interactions, as illustrated in the following section.

3 Localized electrons in molecules

The study of \tilde{P} can be made for ground and excited states equally, as no particular assumptions about the state of the molecule are required for its derivation [10]. This is a practical advantage of the study of our LED over DFT-inspired localization functions, which are valid only for ground states, as imposed by the Hohenberg–Kohn theorem.

In order to get numerical results for molecular systems, we used wavefunctions extracted from Gaussian 09 program (G09) [28] and a modified Fortran code to compute LED. A script that computes LED from cube files generated with the Cubegen routine in G03 is available. All the examples discussed in the present paper were computed at MP2/pVDZ level of theory, unless otherwise stated.

Figure 2 shows the LED graphics for the ground and first excited states of the diatomic hydrogen molecule.¹⁰ The isocontour $\tilde{P} = 0.98$ a.u. for the bonding state of H_2 defines a *valence region* that encloses both nuclei. In the middle, in red, is located the BCP, inside a *covalent region* (orange) given by $\tilde{P} \lesssim 0.3$ a.u. The symmetry of this region indicates that this is a *shared bonding interaction*, that is characterized topologically by a negative Laplacian ($\nabla^2\rho_{\text{BCP}} = -0.7563$, $\rho_{\text{BCP}} = 0.248$ a.u.).

On the other hand, the same valence region for the ungerade state reveals three disconnected surfaces: the two spherical cores centered at the nuclei, and a flat-shaped surface enclosing the BCP. This covalent region (orange) has the shape of a disc located perpendicularly to the gradient path, which is characteristic of a *closed-shell interaction*. Topologically, it corresponds to a positive

¹⁰ Molecular graphics images were produced using the UCSF Chimera package from the Resource for Biocomputing, Visualization, and Informatics at the University of California, San Francisco (supported by NIH P41 RR-01081) [29]. QTAIM computations were done using AIMAll (Version 09.11.08), by Todd A. Keith, 2009 (<http://aim.tkgristmill.com>).

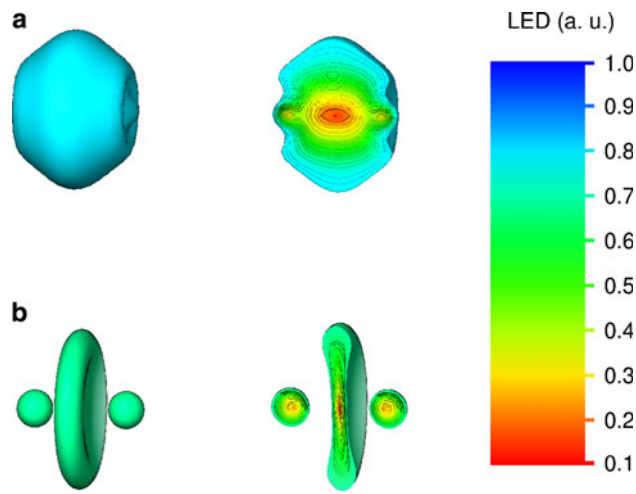


Fig. 2 LED for the ground state (**a**) and the anti-bonding state (**b**) of H_2 at MP2/aug-cc-pVDZ level of theory. The isocontours correspond to $\tilde{P} = 0.98$ a.u. Cross sections are colored as indicated

Laplacian ($\nabla^2 \rho_{\text{bep}} = 1.7246$), and a drop in the electron density to $\rho = 0.124$ a.u., which is characteristic of a non-bonded interaction.¹¹

It is important to state clearly once again that the presence of a bond path is not a sufficient condition to declare that there is a chemical bond between two nuclei, as recently revisited by Bader [30]. In both, the gerade and ungerade states of H_2 , there is a BCP in the middle of the two nuclei, differing by the local symmetries of the electron density which determines the nature of the interaction, i.e. bonded or not bonded, respectively. In the former case, the LED isocontours show that the paired electrons are being shared between the two atoms. For the ungerade state the same isocontour values appear as a set of unconnected spherical shells centered around each nucleus, indicating that the electrons are confined within their respective atomic regions, with an electron density at the BCP that is about twice the electron density at the same distance for the isolated atom.

3.1 Single, double and triple bonded atoms

The 3D plots of \tilde{P} isocontours for the carbon series C_2H_n permit a comparative study of the single ($n = 6$), double ($n = 4$) and triple bonding interactions ($n = 2$). Isocontours at $\tilde{P} = 1.30$ a.u. (yellow) and $\tilde{P} = 0.40$ a.u. (orange) are shown in Fig. 3 for the three molecules.

The BCPs are located at $\tilde{P} = 0$, and therefore the covalent regions around these points depict the bonding interactions. The covalent regions located between the carbon nuclei (in orange) reveal that the single-bonded carbons in

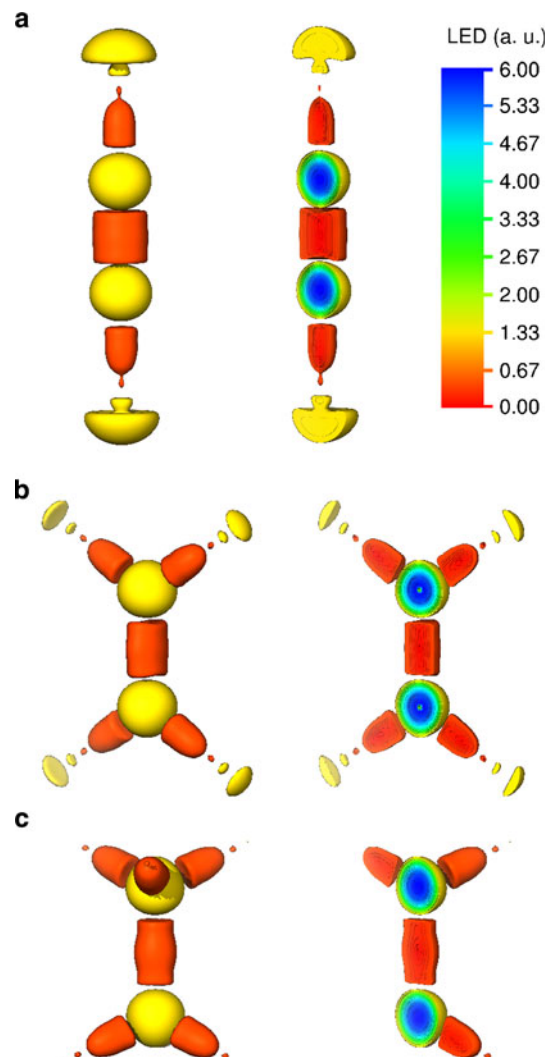


Fig. 3 \tilde{P} isocontours for C_2H_2 (**a**), C_2H_4 (**b**), and C_2H_6 (**c**). Isocontours at $\tilde{P} = 1.30$ a.u. (yellow) and $\tilde{P} = 0.40$ a.u. (orange) are shown for the three molecules. Cross sections are colored as indicated

ethane and triple-bonded carbons in acetylene exhibit cylindrical symmetry, while the double bond of ethylene shows elliptic cylindrical symmetry, with the major axis being perpendicular to the molecular plane (Fig. 3c). The volume enclosed by these covalent regions suggests a progression from single to triple bonded carbons.

A bell-shaped form with the top of the bell toward the hydrogen nucleus characterizes the C–H covalent regions. These isocontours are very similar along the series, as an indication of the transferable character of the C–H bonding interactions.

The cyan, green and blue regions enclosed by the yellow spherical isocontours represent the core electrons of the carbon atoms. These values have a maximum at $\tilde{P} = 6$ a.u., which corresponds to the highest value for the electron

¹¹ For the ground state of H_2 molecule, $\kappa = \tau$ and hence ELF $\eta = 1$ everywhere.

momentum in the neighborhood of a carbon atom, as given by Kato's cusp condition (Eq. 9).

The yellow isocontours located outside the hydrogen bonding regions in Fig. 3 show the electron polarization in the valence region around the hydrogen atoms. Their size decreases from a big semisphere in acetylene to a tiny spheroid for the aliphatic two-carbon alkane, following an inverse order with respect to the C–C bond order of the three molecules.

3.2 Hydrogen bonded systems

The increasing interest in hydrogen-bonded systems has created a need for theoretical tools that can visualize these important types of chemical interactions. ELF fails to provide such information, while the single-particle local momentum correctly detects the presence of hydrogen bonding and provides graphical insight into these systems, as illustrated here.

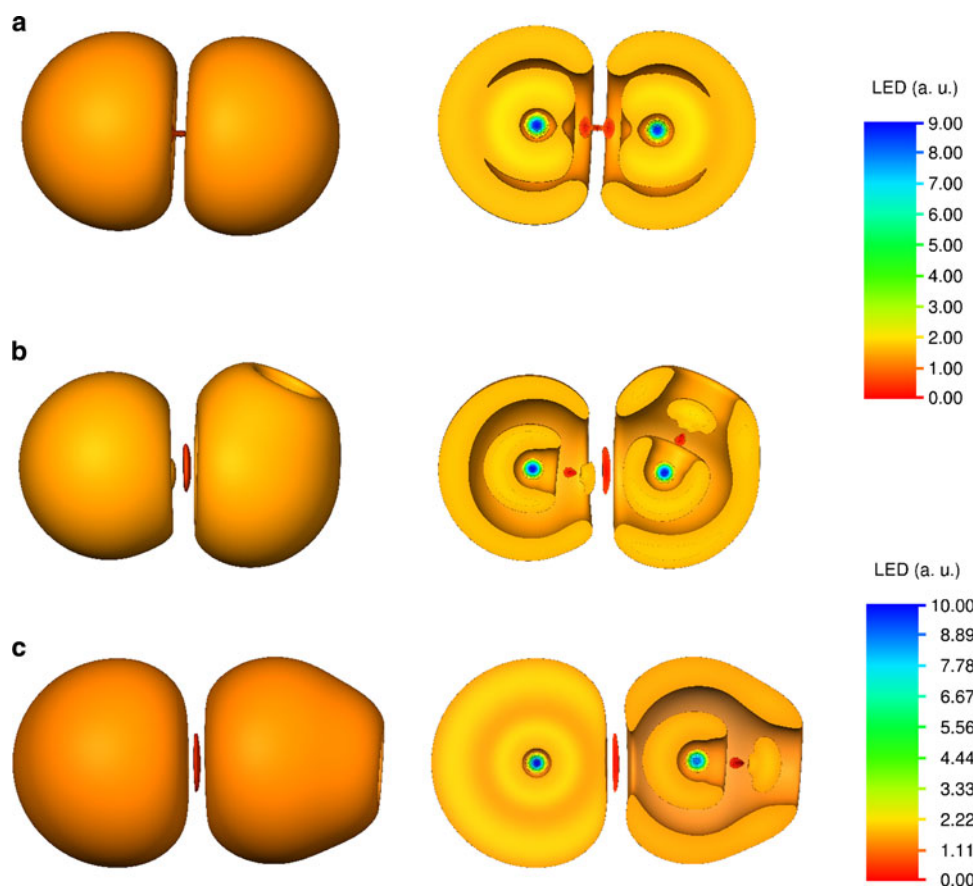
Extreme hydrogen bonding interactions can be adequately studied by the isoelectronic series FHF[−] ion, HF···HF, and Ne···HF, as suggested by Legon [31]. In the ion–molecule complex (FHF)[−], the binding energy borders a covalent bonding interaction with an energy of ~167 kJ/mol [32], while HF···HF is a typical hydrogen bond with a

dissociation energy ~19 kJ/mol dominated by electrostatic forces [33], and in Ne···HF there is a weak interaction with a very low binding energy 3 kJ/mol [34], dominated by dispersive and inductive forces. The LED plots for these three molecules correctly depict the nature of their respective bonding interactions, as shown in Fig. 4.

The valence regions, as given by the isocontours $\tilde{P} = 1.6$ a.u. (dark yellow), reveal significant similarities, in spite of their chemical differences. These contours are disjoint regions, each enclosing a ten-electron subsystem, with greater open sides toward the place where the bonding interactions takes place. The symmetrical shapes of these valence regions suggest an agreement with the premise of VSEPR model, according to which the valence electron pairs surrounding an atom mutually repel each other, and therefore adopt an arrangement that minimizes this repulsion. In Fig. 4 this seems to be true for the inner valence regions located around the atoms in each HF subsystem, as well for the whole complexes. In other words, these results indicate that LED displays the expected behavior of the valence electron pairs.

The covalent regions corresponding to the isocontour $\tilde{P} = 0.6$ a.u. are shown in Fig. 4 in red orange. The covalent region of (FHF)[−] (a) reveals a different character to the other two molecules. In this molecule, each H–F

Fig. 4 LED isocontours for the 20-electrons hydrogen-bonded isoelectronic series: (FHF)[−] ion–molecule complex (a), HF···HF (b), and Ne···HF (c). The covalent regions are in red orange ($\tilde{P} = 0.6$ a.u.) and the valence regions ($\tilde{P} = 1.6$ a.u.) are in dark yellow, according to the LED color key



covalent region resembles more a covalent bond, which can explain its high binding energy, and it is confirmed by the Laplacian value of $\nabla^2\rho_{\text{bcp}} = -1.7208$ ($\rho_{\text{bcp}} = 0.150$), characteristic of a shared interaction.

On the other hand, the hydrogen bonds in the other two molecules show closed-shell interaction features, with $\nabla^2\rho_{\text{bcp}} = 0.1234$, $\rho_{\text{bcp}} = 0.022$ for HF···HF, and $\nabla^2\rho_{\text{bcp}} = 0.0179$, $\rho_{\text{bcp}} = 0.002$ for Ne···HF. This large decrease in the electron density at the BCP (one order of magnitude in each case) is consistent with the hydrogen bond energy strengths.

The cross sections show a conserved character of the HF bonding interaction in these molecules, while the valence shells of those atoms directly involved in the bonding interactions are visibly distorted. The neon atom seems to be only partially polarized in the same direction of the dipole moment of the hydrogen fluoride (c), an indication of the electrostatic nature of this hydrogen bonding interaction.¹²

4 Conclusions

The single particle kinetic energy provides the electronic localization of electron pairs in molecules, and hence its associated momentum $\tilde{\mathbf{P}}$ is an ideal localized electrons detector (Eq. 7). We provide conclusive evidence about how LED depicts the regions where electrons are spatially confined in pairs, as in the case of bonding regions and atomic shells. Unlike \mathcal{D} in ELF, the magnitude of the vector field $\tilde{\mathbf{P}}$, is bounded, has direct (not relative) physical interpretation, and is easily obtainable without knowing the orbital expansion of the electron density. We found that LED isocontours (\tilde{P}) depicts the same kind of symmetries around the BCPs that are given by the Laplacian of the electron density. It means that LED is able to show three-dimensionally the different kinds of bonding interactions identified by the topological analyses: the closed shell and the shared interactions. In the examples discussed here we include QTAIM values of the Laplacian and electron density in order to confirm that the visual depiction provided by LED differentiates these two main bonding interactions, but LED plots can be used as a tool to identify bonding interactions *prior* to any subsequent QTAIM analysis, which is usually a more demanding task.

By studying the single-particle local momentum $\tilde{\mathbf{P}}$, we show that this variable provides a direct analysis of intra and extra molecular bonding interactions. This analysis

agrees with the intuitive notion of the location of bonding interactions in molecules.

Acknowledgments We thank the referees for providing constructive comments and help in improving the contents of this paper. Professors Chérif Matta and Andreas Savin, and our colleague Gavin Heverly-Coulson are gratefully acknowledged for helpful discussions and suggestions. The financial support of the Natural Sciences and Engineering Research Council of Canada and an ACEnet Fellowship, is gratefully acknowledged. Computational facilities are provided in part by ACEnet, the regional high performance computing consortium for universities in Atlantic Canada. ACEnet is funded by the Canada Foundation for Innovation (CFI), the Atlantic Canada Opportunities Agency (ACOA), and the provinces of Newfoundland and Labrador, Nova Scotia, and New Brunswick.

References

- Lewis GN (1916) J Am Chem Soc 38:762
- Hohenberg P, Kohn W (1964) Phys Rev B 136:864
- Bader RFW (1990) Atoms in molecules. A quantum theory. Oxford University Press, New York
- Bader RFW (1994) Phys Rev B 49:13348
- Bader RFW, Johnson S, Tang TH, Popelier PLA (1996) J Phys Chem 100:15398
- Bader RFW, Essen H (1984) J Chem Phys 80:1943
- Becke AD, Edgecombe KE (1990) J Chem Phys 92:5397
- Shi Z, Boyd RJ (1988) J Chem Phys 88:4375
- Silvi B, Savin A (1994) Nature 371:683
- Bohórquez HJ, Boyd RJ (2008) J Chem Phys 129:024110
- Bohórquez HJ, Boyd RJ (2009) Chem Phys Lett 480:127
- Luo SL (2002) Int J Theor Phys 41:1713
- Luken WL, Culberson JC (1982) Int J Quantum Chem 16:265
- Dobson JF (1991) J Chem Phys 94:4328
- Gatti C (2005) Z Kristallogr 220:399
- Silvi B, Savin A (1994) Mineral Mag 58A:842
- Samuelsson P, Büttiker M (2002) Phys Rev Lett 89:046601
- Kohout M, Savin A, Preuss H (1991) J Chem Phys 95:1928
- Cohen L (1996) Phys Lett A 212:315
- Kohout M, Savin A (1996) Int J Quant Chem 60:875
- Navarrete-Lopez AM, Garza J, Vargas R (2008) J Chem Phys 128:104110
- Schmidler HL, Becke AD (2000) J Mol Struct (Theochem) 527:51
- Kato WA (1957) Commun Pure Appl Math 10:151
- Pyykko P (1988) Chem Rev 88:563
- Nguyen-Dang TT, Bader RFW (1982) Physica A 114:68
- Matta CF, Boyd RJ (eds) (2007) The quantum theory of atoms in molecules. From solid state to DNA and drug design. Wiley-VCH, New York
- Site LD (2000) Int J Mod Phys B 14:1891
- Frisch MJ, Trucks GW, Schlegel HB, Scuseria GE, Robb MA, Cheeseman JR, Scalmani G, Barone V, Mennucci B, Petersson GA et al (2009) Gaussian 09 revision A.1. Gaussian Inc., Wallingford
- Pettersen EF, Goddard TD, Huang CC, Couch GS, Greenblatt DM, Meng EC, Ferrin TE (2004) J Comput Chem 13:1605
- Bader RFW (2009) J Phys Chem A 113:10391
- Arunan E, Scheiner S (2007) Chem Int 29:16
- Elgobashi N, González L (2006) J Chem Phys 124:174308
- Klopper W, Quack M, Suhm M (1998) J Chem Phys 108:10096
- Meuwly M, Hutson JM (1999) J Chem Phys 110:8338

¹² In fact this effect is also very small as the dipole moment of Ne···HF is $\mu = 1.963$ D, while the value for HF alone is $\mu = 1.946$ D.